

**POLAR GEOPHYSICAL PRODUCTS DERIVED FROM AVHRR:  
THE "AVHRR POLAR PATHFINDER"**

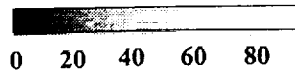
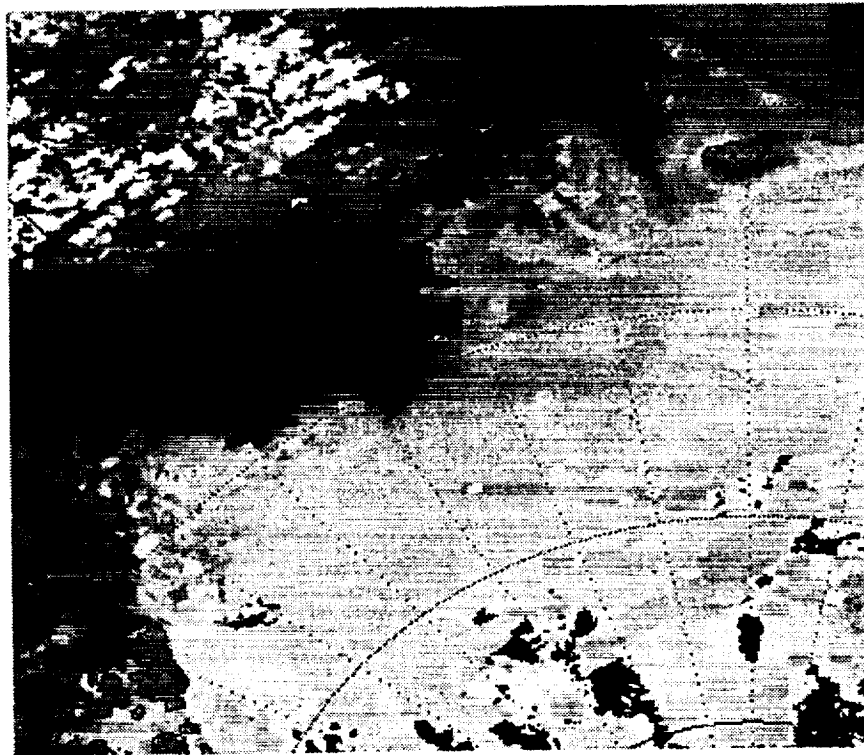
**Final Report**

NAG5-4907

National Aeronautics and Space Administration

December 1999

Principal Investigator:	James Maslanik University of Colorado
Co-Principal Investigators:	Charles Fowler, Theodore Scambos, Jeffrey Key, William Emery
Prof. Research Assistant	Terry Haran



*(Cover figure: Composite of AVHRR Polar Pathfinder clear-sky broadband albedo (%) for July 1998, showing an unusually early and large reduction in Beaufort Sea ice cover)*

**Abstract** This NOAA/NASA Pathfinder effort was established to locate, acquire, and process Advanced Very High Resolution Radiometer (AVHRR) imagery into geo-located and calibrated radiances, cloud masks, surface clear-sky broadband albedo, clear-sky skin temperatures, satellite viewing times, and viewing and solar geometry for the high-latitude portions of the northern and southern hemispheres (all area north of 48° N and south of 53° S). AVHRR GAC data for August 1981 - July 1998 were acquired, with some gaps remaining, and processed into twice-daily 5-km grids, with some products also provided at 25-km resolution. AVHRR LAC data for 3.5 years of coverage in the northern hemisphere and 2.75 years of coverage in the southern hemisphere were processed into 1.25-km grids for the same suite of products. The resulting data sets are presently being transferred to the National Snow and Ice Data Center (NSIDC) for archiving and distribution. Using these data, researchers now have at their disposal an extensive AVHRR data set for investigations of high-latitude processes. In addition, the data lend themselves to development and testing of algorithms. The products are particularly relevant for climate research and algorithm development as applied to relatively long time periods and large areas.

## 1. INTRODUCTION

Analysis of polar climate requires uniform and consistent data sets for monitoring and modeling. A goal of the NASA/NOAA Pathfinder Program is to use currently available Earth information to provide "consistently calibrated global change-related data sets" and to test procedures for generating the consistent data products planned for EOS. To achieve this goal, several Pathfinder efforts have been initiated to address the requirements for integrated and comprehensive data sets for high-latitude climate studies. The AVHRR instruments aboard the NOAA Tiros satellites have been providing daily visible and infrared coverage of the earth since 1981. While the primary purpose of the satellites was for meteorological applications, the data have also been widely used for local areas and over short time periods for case studies of geophysical processes.

Currently there is now an archive of over 19 years of AVHRR Global Area Coverage (GAC) data with a resolution of about 4 kilometers. NOAA and NASA provided funding for the Pathfinder Program to produce a long time series of climatological parameters from these data. Initially, Pathfinder funding was provided for data sets focusing on sea surface and land processes. Subsequently, the NOAA/NASA Pathfinder effort funded several projects to generate data sets tailored for research in high-latitude regions. As a result, polar data from the Pathfinder Program now include products generated from the Tiros Operational Vertical Sounder (TOVS), the Special Sensor Microwave/Imager (SSM/I), and AVHRR. Investigators from each of these high latitude-focused efforts coordinated their projects as much as possible to provide data with a common format, map projection, and file naming convention. The premise of this suite of "Polar Pathfinders" is that: (1) climate studies can best be served by providing a suite of consistent and co-located products that encompass several aspects of the climate system; and (2) these products should be available for a range of scales suitable to different research applications. Here, we describe one component of this "Polar Pathfinder" initiative - the Advanced Very High Resolution Radiometer (AVHRR)-Based Polar Pathfinder ("APP").

The main goals of the APP were to: (1) locate and assemble high-latitude AVHRR coverages for as long a time series as possible, in as consistent and accurate form as possible; and (2) to provide a multiyear series of high-resolution to medium-resolution climate-related products that encompasses several of the key parameters that characterize ice conditions. These include cloud cover, surface temperature and albedo that help define the energy budget of the ice cover, and ice motion information that documents ice dynamical processes over regional to hemispheric scales. A secondary goal of the APP was to also provide reasonably accurate products for open ocean and land surfaces, to facilitate multi-disciplinary studies of processes.

By addressing the task of obtaining, subsetting, and processing AVHRR data into georeferenced, calibrated grids spanning multiyear periods, the products should foster much more extensive applications of AVHRR data than has been feasible in the past. An additional objective is to provide these products in forms compatible with products from Polar Pathfinders such as the TOVS and passive microwave Polar Pathfinders. The availability of the APP products mapped to common grids with these and other data types should encourage the generation of new and "value-added" data sets from combinations with other data sets and from data assimilation within models.

The specific objectives of the APP were:

- locate and assemble Level 1b AVHRR global area coverage (GAC), local area coverage (LAC) and high resolution picture transmission (HRPT) orbital subsets for the polar regions of the northern and southern hemispheres, covering as long a time period as possible;
- Process the entire GAC data as consistently as possible between the several satellites
- Use a gridding scheme that allows comparisons or in combinations with other polar data sets
- generate calibrated and navigated composites of AVHRR at GAC and LAC resolution;
- generate derived geophysical products from these composites.
- Given that improved algorithms will continue to be developed, the individual AVHRR channel data are retained for re-processing

The key tasks to meet these objectives were:

- data acquisition and pre-processing;
- conversion of research-grade software for navigation, calibration, and geophysical algorithms into operational code;
- generation of new software for data selection and compositing;
- production of test data sets;
- refinement of approaches based on test data;
- generation of a suite of sample products for distribution to the user community;
- production runs to generate AVHRR product time series.

This final report describes the procedures used to meet these objectives, and summarizes the resulting products. Portions of this information can also be found in the formal National Snow and Ice Data Center's (NSIDC) Distributed Active Archive Center (DAAC) data set description documentation (DSD). The on-line documentation available from NSIDC will continue to be updated as needed, as will other on-line reports to be provided via the web sites noted below. When possible, results of research and summaries using the APP data will be made available on line to assist users in assessing the potential of the data for their applications.

## 2. PROJECT STATUS

### 2.1 Product Overview (Deliverables)

The AVHRR Polar Pathfinder product suite consists of the following products (additional details are provided below, in the attached appendices, and in the on-line documents):

## Summary of Parameters:

The AVHRR Polar Pathfinder 5 km Data Set contains the following parameters:

- Channel 1 Radiance
- Channel 2 Radiance
- Channel 3 TOA\* Brightness Temperature
- Channel 4 TOA Brightness Temperature
- Channel 5 TOA Brightness Temperature
- Broadband Albedo
- Skin Temperature
- Solar Zenith Angle
- Satellite Elevation Angle
- Sun-Satellite Relative Azimuth Angle
- Surface Type
- Cloud Mask
- UTC of Acquisition
- Ice Motion Vectors

\*Top of Atmosphere

Specifically, the above data sets consist of:

- Subsets of orbital GAC, LAC and HRPT Level 1b data for the regions poleward of 48.4 deg. N and 53.1 deg. S latitude;
- Twice-daily composites at 5 km grid resolution of AVHRR (GAC) channel data, cloud mask, skin temperature, broadband albedo, solar zenith angles; relative azimuth angles; satellite elevation angles; time of pixel acquisition; cloud mask; orbit masks; and surface type masks. The products are gridded on the Equal Area Scaleable Earth-Grid (EASE-Grid). Composites are created for 0400 and 1400 local time for the Northern Hemisphere and at 0200 and 1600 for the southern hemisphere;
- Twice-daily composites of the above parameters mapped to a 1.25-km grid and obtained from LAC and HRPT data;
- Reduced resolution ("browse") versions of the 5-km products averaged to a 25 km grid spacing;
- Grids of sea ice displacement vectors for the polar regions, consisting of separate vector sets from AVHRR 5-km and 1.25-km data, Scanning Multichannel Microwave Radiometer (SMMR), and Special Sensor Microwave Imager (SSM/I), and a blended ice motion product including these data sets for the Antarctic, and including these buoy displacements from the International Arctic Buoy Program (IABP) for the Arctic.
- Documentation describing data set characteristics and processing procedures.
- Data examples and documentation available on an NSIDC web site, and provided for inclusion on a "sampler" CD being prepared by NSIDC.

The following processing has been completed:

- Acquisition of GAC Level 1b data for 8/1981- 12/1993 - 7/1998, excluding 1994;
- Generation of high-latitude subsets for the above period, but also excluding 1996;
- 5-km navigated, calibrated and composited channel data and ancillary data grids for the above periods, excluding 1994 and 1996.
- 5-km skin temperature, broadband albedo, and cloud mask grids for same;
- 25-km browse products for same;
- LAC/HRPT subsets for 1995-1998;
- Ice motion data from 5-km AVHRR imagery for 1986-1989, 9/1997-2/1998;

- 1.25-km navigated, calibrated and composited channel data and ancillary data grids for 8/1993 - 8/1994, 2/1995-10/1995, 1997 - 1998 for the northern hemisphere, and 4/1992-1/1995, and 1/1996 for the southern hemisphere;
- Ice motion data from 1.25-km AVHRR imagery for the above period;
- SMMR- and SSM/I-derived ice motion data for 1979-1998 (both hemispheres);
- Visualization products including animations of 25-km time series.

The above products represent approximately 2.2 terabytes of data processed for the GAC subsets, 1.5 terabytes of composited products at 5-km resolution, and 5.5 terabytes of composited products at 1.25-km resolution. The time period covered by the 5-km products is approximately 1.5 years longer than originally proposed.

In addition to the software development, data analysis, and processing tasks that were necessary for product generation, we also developed a prototype of an "on-demand" APP processor for use at NSIDC. This system allows the APP processing steps to be applied to all individual AVHRR swaths covering a region, and can be used to generate APP products for any time period within the LAC/HRPT coverage available at NSIDC. It is planned that this system will be continually updated to incorporate improvements in algorithms and processing.

## *2.2 Difficulties Encountered and Uncompleted Tasks*

By the end of the project, several tasks, as reviewed below, remain uncompleted. Some will be finalized in the normal course of ongoing work, while additional funding may be requested to support the more intensive efforts.

While the AVHRR- and passive microwave-derived ice motion products are complete or essentially complete, the merged products had not yet been generated by the project end date. We anticipate completing these ice motion data under other related funding within the next two months, with the data to be delivered to NSIDC.

The remaining large data gaps are due to the fact that GAC data for 1994 and 1996 were not available until late in the project. We are now able to obtain these data from the NOAA Satellite Active Archive (SAA). We intend to pursue additional funding to fill these time gaps as well as smaller gaps scattered throughout the time series.

The APP processing itself was delayed for several reasons. First, data availability hampered initial processing. No one location had all the GAC data. Thus, it was necessary to acquire data from several sources, which entailed considerable additional effort to address different distribution mechanisms, contacts, and media. This resulted about a six-month delay. The problems were overcome through the much-appreciated assistance from several individuals and organizations.

Calibration also presented more problems than expected. While we are aware that calibration of AVHRR remains an uncertain issue and that calibration methodologies were not designed with the particular goal of facilitating long time series analysis, the uncertain and continually involving state of the calibrations led to the need for some re-processing. Initially, the most current available calibration information was used. Late in the project, a different procedure became available for NOAA-14. At that time, the calibration of the AVHRR data from all the NOAA satellites was updated to this new method. This method attempts to better calibrate the data over a wider range of temperatures. Previously, calibrations were optimized for ranges suitably for ocean temperatures. Also, within the last year, NOAA-14 visible calibrations were redone to accommodate the most current assessment of instrument drift. We concluded that implementing these revised calibrations could substantially improve the APP products. The resulting coding changes, analyses, and re-processing resulted in a delay of about 2 months.

Two unanticipated problems arose in the production of the APP final products. First, although test cases did not reveal particularly large errors in the geophysical products, errors became increasingly apparent once a longer time period of the APP data was

generated. In particular, unacceptable deficiencies were detected in the albedo algorithm.. These errors were found when comparisons and validation studies were done, when results for a number of regions were inter-compared, and when results from different NOAA satellites could be examined. Errors were not unexpected, since the algorithms had been developed from a limited amount of data. However, the APP products required knowledge of a wider range of conditions such as solar zenith angles and atmospheric path lengths. The algorithms were subsequently improved to better address the wide variety of conditions encountered within the APP coverages. While we believe that the resulting data are of an acceptable accuracy for many purposes, additional improvements will certainly result from further research. It is worth noting that the gridded radiances generated by the APP project will greatly facilitate such algorithm development and testing.

Cloud detection and masking also proved less accurate than desired, with some rather large errors encountered in some regions and conditions. Again, algorithms had been developed based on limited data sets. When applied to the wider coverage necessary for the hemispheric extent of the APP processing, many conditions caused either clear areas being classified as cloudy, or vice versa. An additional method of cloud detection was added that capitalizes on the availability of the AVHRR time series, and the results of three cloud-detection options are being included in the APP cloud mask. These improvements are being applied as the data are being delivered to NSIDC.

Overall, the testing and implementation of the improved algorithms added about 6 - 9 months to the final processing time, and involved re-processing 11 years' worth of GAC data. In total, more than 1 year was added to our initial estimates of processing time. Despite this delay and the added effort for re-processing, we believe that the quality of the resulting products justify the extra effort and time required.

### *2.3 Sources of Additional Information*

This report provides an overview of the main tasks and results from the APP effort. Since we are continuing to expand and update the user documentation, readers and in particular, data users, are encouraged to see the following web sites for the latest version of this report, status reports on processing and ingest at NSIDC, descriptions and examples of the products, visualization products, and data samples, including NSIDC product documentation and information for obtaining the data. Some specific information not contained here, such as definitions of the data values associated with contents of the surface and cloud masks, is provided in the NSIDC documents.

(NSIDC home page, with links to APP guide documents and data ordering procedures):  
<http://www-nsidc.colorado.edu>

(Status reports and other detailed information on APP processing, including some sample data):  
<http://www-nsidc.colorado.edu/PROJECTS/PATHFINDER/>

(Portions of the Polar Pathfinder sampler CD prepared by and available from NSIDC):  
[http://www-nsidc.colorado.edu/NASA/POLAR\\_PATHFINDERS/PCUBE/index.htm](http://www-nsidc.colorado.edu/NASA/POLAR_PATHFINDERS/PCUBE/index.htm)

(Home page for CCAR APP 5-km APP processing. Also related papers and reports):  
<http://polarbear.colorado.edu>

(Detailed description of the map projection used):  
[http://www-nsidc.colorado.edu/NASA/GUIDE/EASE/ease\\_maps\\_info.html](http://www-nsidc.colorado.edu/NASA/GUIDE/EASE/ease_maps_info.html)

(Detailed descriptions of CASPR algorithms and processing steps)  
: <http://stratus.ssec.wisc.edu/caspr/caspr.html>

Additional information will continue to be placed on these sites, with revised and updated user documentation. Further discussion of the APP products can be found in the following publications that have been supported in part by this project:

- Hutchinson, T.A. and T.A. Scambos, 1997. High-resolution polar climate parameters derived from 1-km AVHRR data, Am. Met. Soc., 8th. Conf. on Global Change Studies, 284-291.
- Meier, W.N., J.A. Maslanik, J.R. Key, and C.W. W. Fowler, 1997. Multiparameter AVHRR-derived products for Arctic climate studies, *Earth Interactions*, Vol. 1.
- Maslanik, J., C. Fowler, J. Key, T. Scambos, T. Hutchinson, and W. Emery, 1998. AVHRR-based Polar Pathfinder products for modeling applications. *Annals of Glaciol.*, 25, 388-392.
- Maslanik, J.A., A. Lynch, and C. Fowler, 1999a. Assessing 2-D and coupled-model simulations of sea ice anomalies using remotely-sensed polar pathfinder products, Fifth Conference on Polar Meteorology and Oceanography, Am. Met. Soc., Dallas, TX, 10-15 January, 476-479.
- Maslanik, J.A., J. Key, C. Fowler, T. Nguyen, and X. Wang, 1999b. Spatial and Temporal Variability of Satellite-derived Cloud and Surface Characteristics During FIRE-ACE, submitted to *Journal of Geophysical Research*, November, 1999.

### 3. PROCESSING AND PRODUCTS

The APP data set includes twice-daily navigated and calibrated grids of radiances, satellite viewing angles, and derived products. The data set covers both poles and comprises the following variables: composites of albedo and surface (skin) temperature (at 0400 and 1400 for the northern hemisphere, and at 0200 and 1600 for the southern hemisphere); calibrated channel data from each of the five channels; solar zenith angles; relative azimuth angles; satellite elevation angles; time of pixel; cloud mask; orbit masks; and surface type masks. AVHRR GAC are used to generate APP products at grid spacings of 5 km x 5 km, and reduced-resolution versions of the 5 km products (albedo, skin temperature, viewing angle, time, and cloud mask) at 25 km x 25 km. LAC and HRPT data are used to generate products at 1.25-km resolution. The albedo, ice surface temperature, and cloud masks are provided for these various grid cell sizes to accommodate uses ranging from detailed process studies to climate model validation.

Figure 1 summarizes the basic AVHRR processing for the GAC-based (5-km) products. The processing procedure for the 1.25-km products is similar, and algorithms and products are equivalent except where otherwise noted (and where differences arise from spatial resolution). The NSIDC documentation provides additional details on remaining differences associated with the two product types. Details of the processing are provided below and in the appendices.

# AVHRR GAC PROCESSING

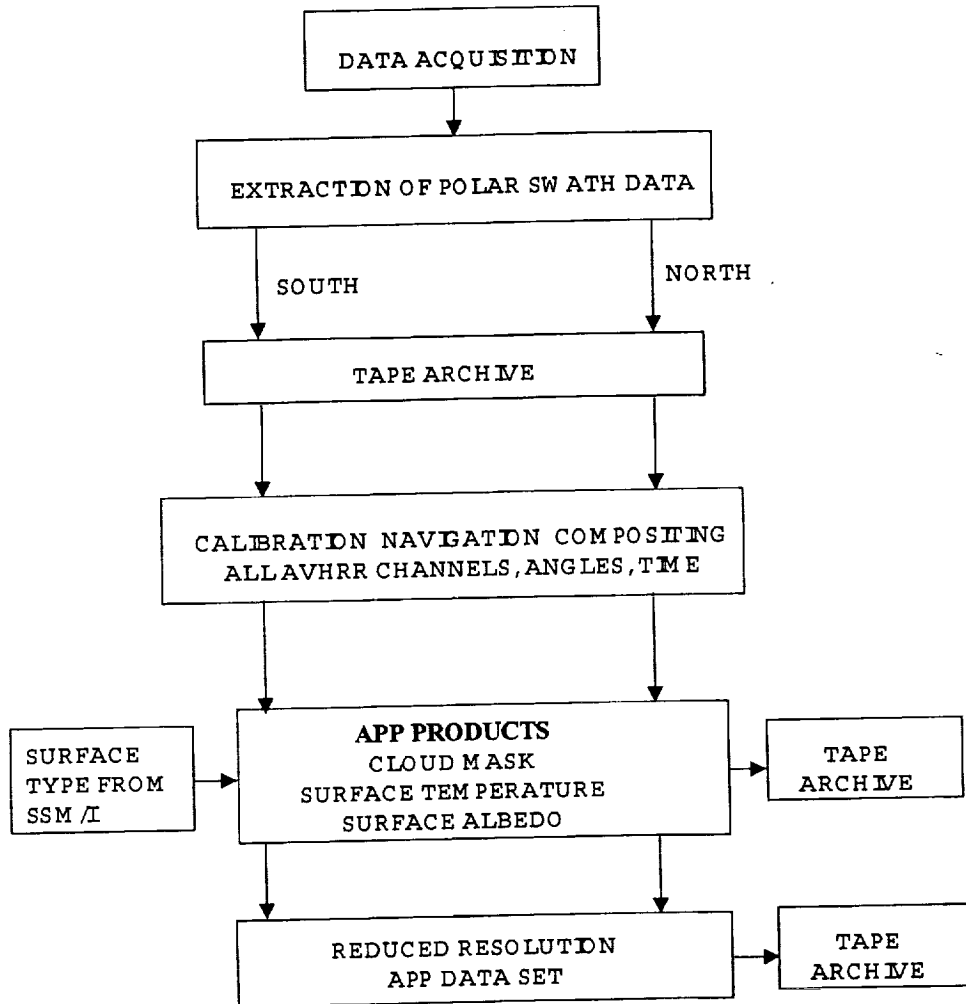


Figure 1. Basic processing steps of the AVHRR Polar Pathfinder (APP).

### 3.1 Data Set Description

The APP product coverage is given in Table 1. These products are gridded on the Equal Area Scaleable Earth-Grid (EASE-Grid) (*Armstrong and Brodzik, 1995*). The spatial coverage extends poleward of 48.3 deg. N and 53.1 deg. S latitude at the edges of the grids and approximately 12 degrees further equator-ward at the grid corners. Figures 2 and 3 illustrate the areal coverage for the northern and southern hemispheres. Products and the associated volume, bit depth, and scaling are given in Tables 2 and 3.

Table 1. AVHRR-Based Polar Pathfinder Products.

Product	Coverage Period	Cell Size
GAC polar subsets	8/1981 - 7/1998	native GAC
Navigated and calibrated composites of channels 1-5 radiances	8/1981 - 7/1998*, twice daily 8/1993 - 8/1994, 2/1995-10/1995, 1997-1998 for the northern hemisphere, 4/1992-1/1995, and 1/1996 for the southern hemisphere twice daily	5 km  1.25 km
Viewing angles and pixel acquisition times	8/1981 - 7/1998, twice daily (above dates), twice daily	5 km 1.25 km
Surface albedo, skin temperature	8/1981 - 7/1998, twice daily (above dates), twice daily	5 km, 25 km 1.25 km
AVHRR ice motions	8/1981 - 7/1998, daily (above dates), daily	50 km 25 km
Blended ice motions (AVHRR, buoys, SMMR, SSM/I)	8/1981 - 7/1998, daily	62.5 km

\* dates given are for both hemispheres for the 5-km products.

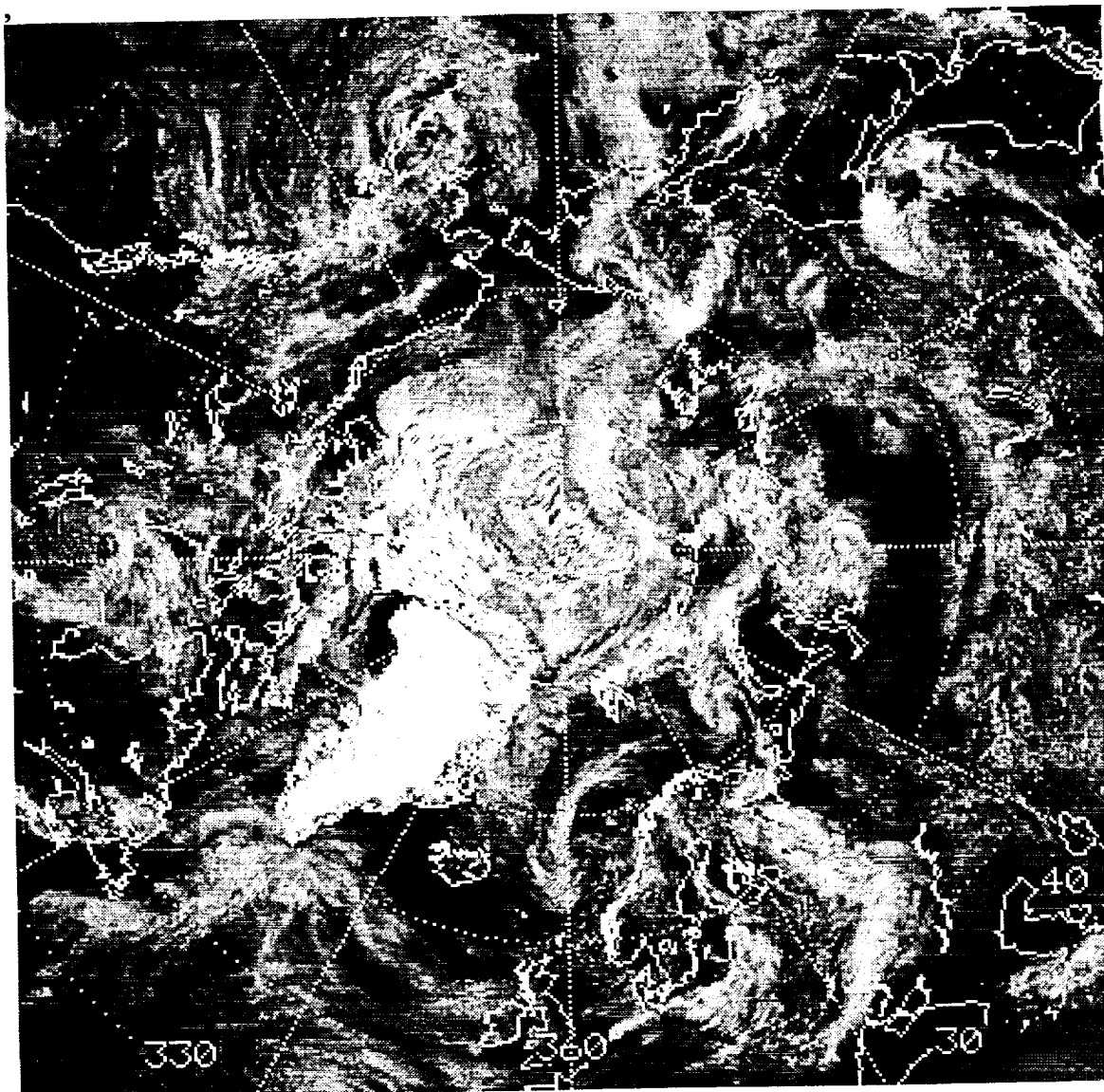


Figure 2. Sample AVHRR composite of 5-km broadband albedo data for the northern hemisphere at 1400 local time on 8 September 1997, illustrating the northern hemisphere data coverage.

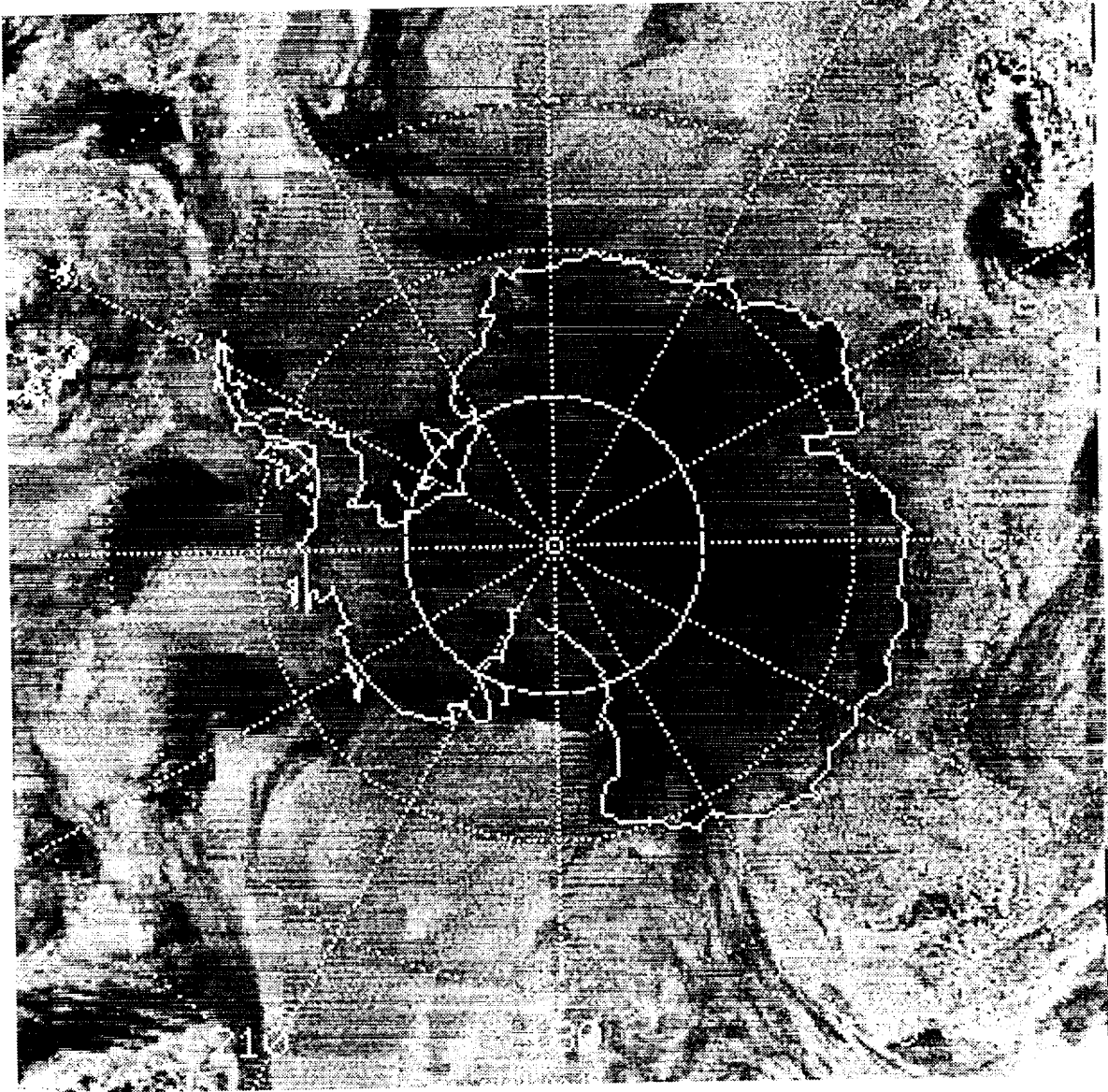


Figure 3. Sample AVHRR composite of 5-km skin temperature data for the southern hemisphere at 0200 local time on 8 September 1997, illustrating the southern hemisphere data coverage.

Table 2. Summary of 5-km APP products.

<b>AVHRR 5 km Data Set Products and Data Volumes (for both hemispheres)</b>					
Product	bytes/pixel	times/day	MB/day	units	scaling factor
Channel 1 Radiance*	2	2	23	% albedo	0.1
Channel 2 Radiance*	2	2	23	% albedo	0.1
Channel 3 TOA Brightness Temperature	2	2	23	Kelvin	0.1
Channel 4 TOA Brightness Temperature	2	2	23	Kelvin	0.1
Channel 5 TOA Brightness Temperature	2	2	23	Kelvin	0.1
Broadband Albedo	2	2	23	% albedo	0.1
Skin Temperature	2	2	23	Kelvin	0.1
Solar Zenith Angle	2	2	23	Degrees	0.1
Satellite Elevation Angle	2	2	23	Degrees	0.1
Sun-Satellite Relative Azimuth Angle	2	2	23	Degrees	0.1
Surface Type	1	1	6	N/A	N/A
Cloud Mask	1	2	12	N/A	N/A
UTC of Acquisition	1	2	12	Hour	0.1
Ice Motion Vectors	N/A	1	2 maximum	cm/sec	N/A
<b>TOTAL</b>	<b>260 MB/day</b>				
<p>* In the nomenclature of NOAA documentation (Kidwell K. B. 1991) "radiance" refers to TOA spectral albedo.</p> <p>Data have been scaled (except surface type and cloud mask, indicated by N/A), by applying a scaling factor. The original data values can be recovered using the following equation:  <math>orig\_value = Scaling\_Factor \times (scaled\_value)</math>.</p>					

Table 3. Summary of 1.25-km APP products

<b>AVHRR 1.25 km Data Set Products and Data Volumes (for both hemispheres)</b>					
Product	bytes/pixel	times/day/hem	MB/day	units	scaling factor
Channel 1 Radiance*	2	2	373	% albedo	0.1
Channel 2 Radiance*	2	2	373	% albedo	0.1
Channel 3 TOA Brightness Temperature	2	2	373	Kelvin	0.1
Channel 4 TOA Brightness Temperature	2	2	373	Kelvin	0.1
Channel 5 TOA Brightness Temperature	2	2	373	Kelvin	0.1
Broadband Albedo	2	2	373	% albedo	0.1
Skin Temperature	2	2	373	Kelvin	0.1
Solar Zenith Angle	2	2	373	Degrees	0.1
Satellite Elevation Angle	2	2	373	Degrees	0.1
Sun-Satellite Relative Azimuth Angle	2	2	373	Degrees	0.1
Cloud Mask	1	2	187	N/A	N/A
Orbit Mask	1	2	187	N/A	N/A
UTC of Acquisition	1	2	187	Hour	0.1
Ice Motion Vectors	N/A	7 maximum	100 maximum	cm/sec	N/A
<b>TOTAL</b>	<b>4391 MB/day</b>				
<p>* In the nomenclature of NOAA documentation (Kidwell K. B. 1991) "radiance" refers to TOA spectral albedo.            Data have been scaled (except cloud and orbit masks, indicated by N/A), by applying a scaling factor.            The original data values can be recovered using the following equation: <math>orig\_value = Scaling\_Factor \times (scaled\_value)</math>.</p>					

### 3.2 Data Acquisition

The data are acquired by the AVHRR multispectral scanner carried onboard the Tiros series of NOAA satellites. There are usually 2 satellites in orbit at any given time, a "morning" and an "afternoon" satellite. This time designation refers to the approximate time the satellite crosses the equator. For the APP, only the afternoon satellites were used. The data coverage for NOAA-7 begins in the summer of 1981 and continues to the present, with satellites NOAA-9, NOAA-11, and currently with NOAA-14. The Tiros satellites are sun-synchronous with equator crossings are about the same local solar time each day. The satellites are polar orbiting with an inclination of about 98 degrees, with about 14 orbits per day.

The AVHRR instrument providing the data used here is a 5 channel scanning radiometer. The channels range from visible to infrared wavelengths. There are 1024 scans each scan line with scan angles +/- 55 degrees. The resolution of the instrument is 1.1 Km at nadir and about 8 Km near the edges of the scan line. This coverage provides a slight overlap at the equator and 100% overlap at the poles between consecutive orbits. There is then complete sensor coverage of every location on the Earth twice per day during both ascending and descending portions of the satellites' orbits.

The AVHRR data delivery system operates in 3 modes. First is the High Resolution Picture Transmission (HRPT), with the satellite transmitting real-time data at the full resolution. The second mode is LAC, having the full resolution data being recorded for later download. The LAC is a by-request mode and varies by orbit. The data recorders aboard the Tiros satellites are not able to completely record all the sensor data at full resolution. To address this, a third mode, GAC, is recorded reduced resolution. The reduction is done by averaging 4 scan spots and ignoring the 5<sup>th</sup> field of view along each scan line, and then only recording every third scan line. The resolution of the GAC data is usually considered to be about 4 km.

The GAC and LAC data from the on-board data recorders are downloaded to 2 locations, Wallops Island, Virginia, and Gilmore Creek, Alaska. There are several separate data recorders aboard each satellite. Before download begins, another recorder begins recording, so that there is some overlap in the data. The first recorder is stopped, rewound, and downloaded. The majority of the AVHRR data is downloaded to the Gilmore Creek site because of its geographic location. Most of the GAC data have overlaps and are not continuous orbital swaths in the Arctic region.

For the APP 5 km processing, GAC data in level 1b format were obtained from a variety of sources, including the Jet Propulsion Laboratory (JPL) Physical Oceanography Distributed Active Archive System (DAAC), the National Center for Atmospheric Research, the Goddard Space Flight Center DAAC, the Colorado Center for Astrodynamic Research (CCAR) DOMSAT facility at the University of Colorado, and the NOAA Satellite Active Archive Center (SAA). Since August of 1993, NSIDC has collected and archived a polar data set of 1 km HRPT and LAC AVHRR imagery from several HRPT receiving stations, most importantly McMurdo, Palmer, Casey, Fairbanks, Prince Albert, and Tromsø, and from recorded and rebroadcast LAC images for both polar regions. Most of the data are obtained as a polar subset of the Global Land 1 km AVHRR Data Set currently collected and distributed by the EROS Data Center (EDC). Antarctic HRPT data from the McMurdo and Palmer receivers are collected by Scripps Institute of Oceanography. LAC data of the southern hemisphere is provided, in part, by the University of Colorado DOMSAT receiver.

Each source provided the data in different formats on different media. One year of GAC data (1992) had been provided from JPL on Exabyte tape for a previous project. This data was used to develop the APP processing system and testing of the algorithms. Four years (1988-1991) were obtained from GSFC also on Exabyte tape. A special processing system was set up to duplicate data from JPL. The media was large storage platters that

could only be read with a reader that was loaned to us by JPL. This required a Digital Equipment machine computer running the VMS operating system. Mr. V. Troisi and others at NSIDC provided invaluable assistance in transferring these JPL platters to DLT tape for subsequent APP processing. In addition to these sources, approximately 1.5 years of GAC data were obtained via the C.U. DOMSAT facility. The remaining GAC data were obtained from NOAA's SAA. Their mission statement only allows them to disseminate data over the internet. We were able to make special arrangements for downloading about 40 Gbytes of data on a daily basis. All the LAC and HRPT data used for the 1.25-km processing were provided by NSIDC.

### 3.3 Data Processing and Product Description

#### 3.3.1. Extraction and compositing of channels 1-5 radiances

Once the data were obtained and copied to tape, the first step in the processing was to extract the orbital data for the polar regions from the global Level 1b swaths. Because much of the recorded GAC data is downloaded at the NOAA station at Gilmore Creek, Alaska, most of the Arctic data have starts and stops with some overlaps (e.g., recorded orbit cycles begin and end over the Arctic). It was necessary to "stitch" data pieces together with redundant data removed, to yield full Arctic passes. These subsets were then saved to 8mm tape in Level 1b format.

Data were extracted from particular orbits to best match a set of decision criteria defined by the satellite scan angle and the acquisition time in relation to "target times." These criteria were selected to choose data close to the target times while minimizing scan angles (to reduce algorithm errors due to atmospheric path length and bi-directional reflectance and to maximize spatial resolution). The selected data for the five AVHRR channels were then assembled into two composites per day, for local times of 0200 and 1600 GMT for the Southern Hemisphere and 0400 and 1400 GMT for the Northern Hemisphere. Because of the orbital path, the times cannot be 12 hours apart. These times were also chosen to be as consistent as possible over the life of the individual satellites, and required taking into account the drift of the equator crossing times of the satellites (Figure 4). Figure 5 shows the scan angle based upon the compositing criteria. As indicated, the

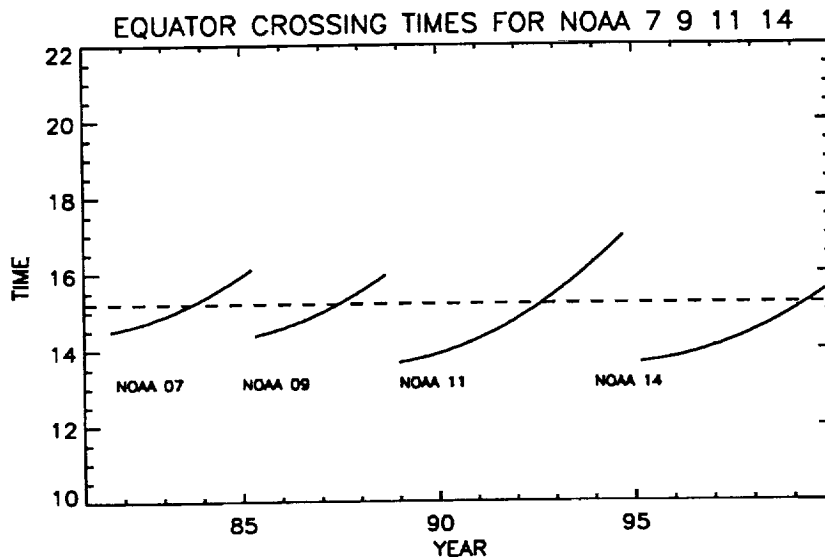
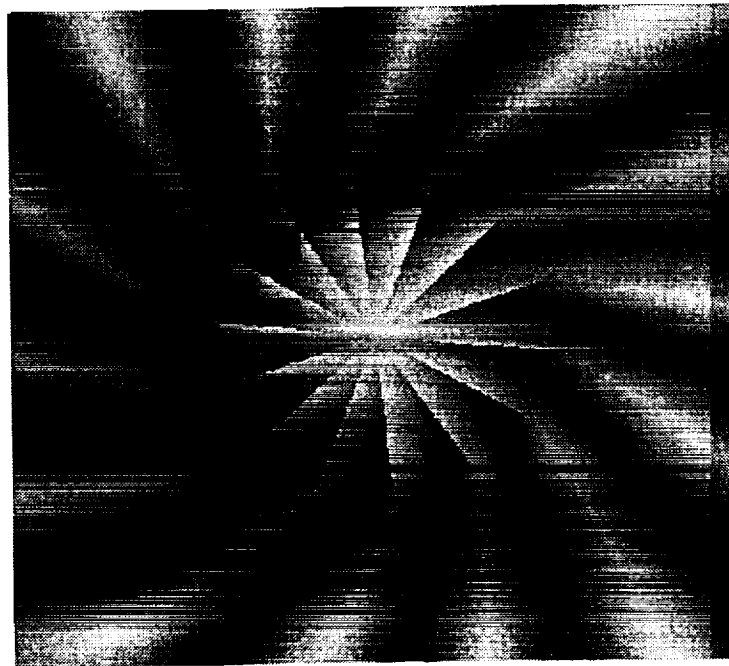
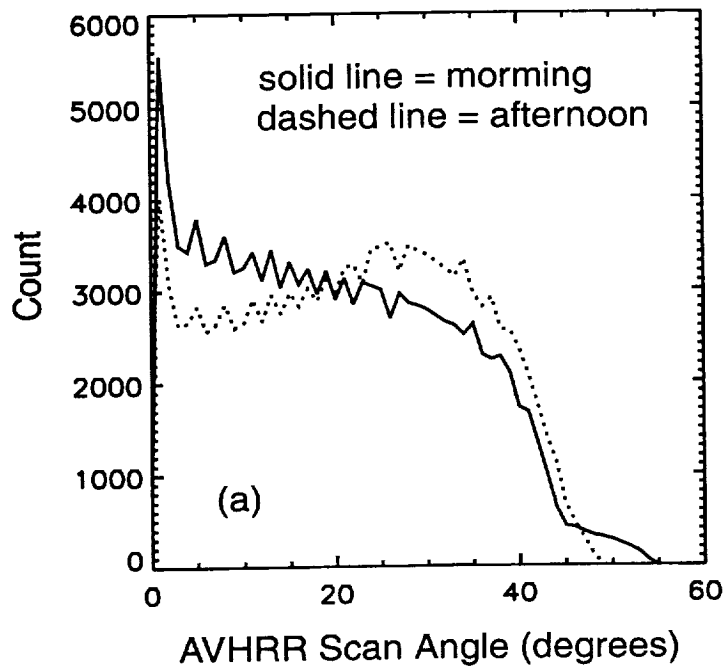


Figure 4. Drift of equator crossing times over the life of the AVHRR satellites.



(b)

Figure 5. Histogram showing count of pixels versus scan angle for the morning and afternoon composites (a). Scan angle is plotted as an image in (b). Nearer the pole, higher scan angles are necessary due to the orbit inclination of the satellite. Here, NOAA 9 data for 2 January 1988 are used as an example.

majority of the pixels are acquired at the desirable low scan angles. For the southern hemisphere, the choice of target time is restricted by the fact that the satellite is passing over the south polar area at a later local time, meaning that more of the satellite data used for compositing will be past the terminator. This dictated the choice of 0200 and 1600 GMT for the southern hemisphere target times. The precise local time for 90% of the cells in each grid is within 1 hour of the target time, and 90% of the cells are acquired with scan angles less than 25 degrees.

### 3.3.2 Navigation and calibration

The next steps in the processing are the calibration of the level 1b data and navigating (geolocating) to the EASE grid. While the GAC data have embedded calibration and geolocation information, our own geolocation and calibration software was used to calculate new calibrations and positioning. The GAC data have been produced at different times and have different versions of calibration, and it was necessary to use the most current methods. As noted below, improvements were also possible using our navigation routines.

Channels 1 and 2 are calibrated using coefficients developed by the NOAA/NASA AVHRR Pathfinder Calibration Working Group. Non-linear calibrations obtained from NOAA are applied to channels 3, 4 and 5 (e.g., *Rao et al., 1993*). During the APP program, calibration methods have changed, necessitating changes in the processing. One problem has been that the AVHRR calibration has been historically optimized for sea-surface temperatures. The polar regions required a wider temperature range. Also, the polar regions have unique problems with very low sun angles and calibration is very important. The original calibrations were applied to a portion of the data processed early in the project. The method mentioned above by *Sullivan et al. (1999)* and *Rao and Chen (1999)* were later implemented for the channels for all the AVHRR satellites. The change over occurred in March, 1999. The composited radiance files are thus designated as version 1 or version 2. Version 1 data were processed using the original calibrations but with a subsequent set of corrections noted below, with version 2 data processed using the improved calibrations that became available near the end of the project.

To improve the calibration of the version 1 data, correction tables were generated for these previously processed data to match as closely as possible the new calibration techniques. These corrections appear to be compatible within 0.0 +/- 0.1 degrees. Additional information and discussion of the calibration procedures are given in Appendix 1.

Calibration yields raw albedo values (spectral albedo) for channels 1 and 2, and brightness temperatures for the thermal channels. These calibrated data were then navigated to earth coordinates using an orbital ephemeris model with orbit and clock time corrections (*Rosborough et al., 1995*). Satellite ephemeris used is obtained from the Naval Space Surveillance Center (NAVSPASUR). A forward navigation approach is used to assign pixels to individual grid cell locations. In this approach, the geographic latitude and longitude locations of the grid are mapped to the corresponding scan line and sample in the input data. Using this method, no interpolation or averaging in time or space is applied to the resulting gridded data. Geolocation accuracy is typically sub-pixel (approximately 2 km for the 5-km processing).

The resulting data grids are 1805 x 1805 pixels (northern hemisphere) and 1605 x 1605 pixels (southern hemisphere) for the 5-km products, and 7220 x 7220 and 6420 x 6420 pixels respectively for the 1.25-km products. As indicated in Tables 2 and 3, most data types are stored as 16-bit integers, with data values multiplied by 10. Total data volume for the complete set of 5-km products per day (both hemispheres) is 154 MB (excluding and 2457 MB for the 1.25-km data

These first two stages of processing - assembling and extracting the Level 1b subsets followed by navigation and calibration - comprised nearly 80% of the processing

effort for the APP, and have long been the most difficult tasks for individual users to perform.

### 3.3.3 Solar Zenith Angle, Relative Azimuth Angle, and Satellite Elevation Angle

A set of viewing and illumination angles is provided for each pixel, as calculated from the satellite ephemeris. These angles can be used to investigate angular effects, and to test or apply alternative bi-directional reflectance distribution function adjustments for derived products. All angles are stored at 16-bit integer data. Angles are multiplied by 10 to scale them to within the 16-bit data range. Solar zenith angle is the angle of the sun from nadir (e.g., 90-solar zenith angle = angle of the sun above the horizon). Relative azimuth angle is the solar azimuth angle minus the satellite azimuth angle. Satellite elevation angle is the scan angle of the AVHRR from nadir for the particular pixel (e.g., the viewing angle for that pixel).

### 3.3.4 Time tag

An acquisition time is provided for each pixel. The time is stored in a 16-bit integer as hour (GMT) times ten. The acquisition time is thus known to within +/- 6 minutes for each pixel.

### 3.3.5 Surface type mask

As part of the cloud masking step, different inputs to the masking can be supplied depending on whether the surface is considered to be open ocean, ocean with sea ice cover, snow-covered land, or bare land. Defining the surface type allows the cloud detection procedure to be adjusted for different surface conditions. Figure 6 shows the main processing steps associated with this mask generation.

For the APP, SMMR and SSM/I data are used to partition the surface into open water, sea ice, snow-free land, snow-covered land, and land covered by ice sheets. The brightness temperatures used are those distributed by NSIDC on the SSM/I polar stereographic grid, and then re-mapped to the EASE grid projection. The presence of snow cover over land is flagged using these SMMR and SSM/I brightness temperatures and the basic algorithm used as part of the SSM/I Polar Pathfinder snow cover products. Over ocean areas, the NASA Team Algorithm was used to generate concentrations of first-year and multiyear ice. For the purposes of the cloud detection procedure, all ocean pixels with an estimated ice concentration greater than 0% were flagged as "sea ice". It is known that atmospheric effects and wind-roughening of the ocean cause false retrievals of ice concentration over open ocean in some cases. Such areas will appear as incorrectly-mapped areas of sea ice in the mask, but for cloud detection, preliminary work suggests that it is important to avoid excluding areas with true ice cover less than 15%. Areas estimated by the NASA Team algorithm to consist of at least 50% multi-year ice are assigned the "multi-year ice" flag. The mask identifies ranges of ice concentration, which can be used to help identify areas subject to errors associated with the presence of a small fraction of ice.

A gradient value (G) greater than zero is taken to indicate presence of snow, and the pixel is assigned a "snow" surface type. No special thresholds are applied, nor are special cases such as melting snow addressed in this mask. This 5-km mask is over-sampled from the 25 km SMMR and SSM/I data. See the on-line NSIDC data set document for information regarding the nature of the surface type mask, and the information content of the surface-type and cloud masks.

The applications of the passive microwave algorithms for sea ice and snow as used here are intended only for the relatively coarse purposes of ascribing general surface types for the AVHRR product generation. Users interested in specific analyses of ice and snow

conditions from the microwave data should make use of the more thoroughly documented and tested sea ice and snow products available from NSIDC.

### SURFACE TYPE FROM PASSIVE MICROWAVE DATA

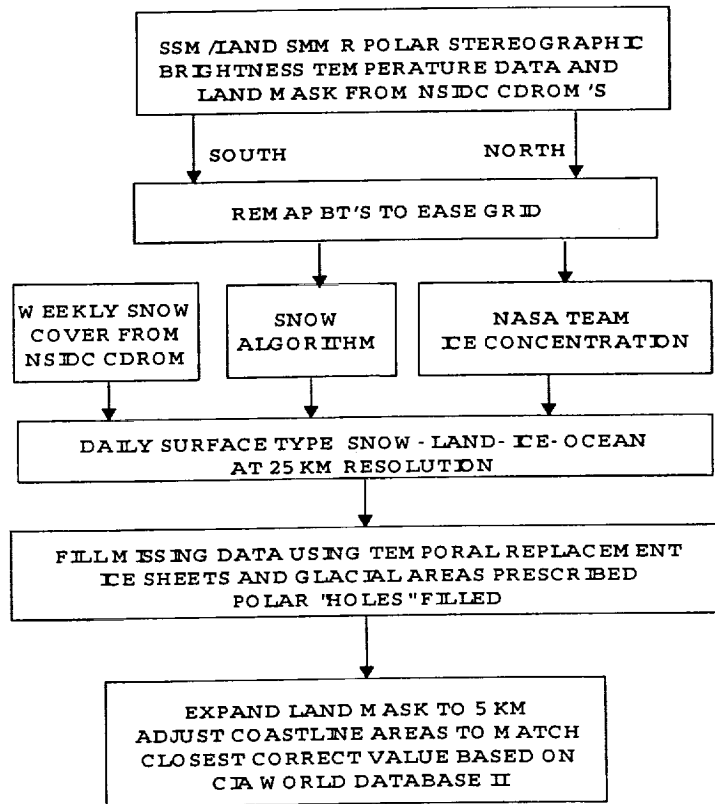


Figure 6. Processing steps to generate the surface type masks used for APP product generation.

#### 3.3.6 Cloud Detection and Mask

The cloud detection methods used for the APP are optimized for polar conditions. Given the importance of the cloud masking step, and the difficulties involved, a considerable amount of work was dedicated to testing and refining the cloud detection procedure used. In particular, the methods had to be able to address a wide range of conditions since the spatial coverage of the APP data encompass essentially global conditions ranging from snow-free, warm land to the coldest regions of the earth. In addition, cloud detection is greatly hampered by the lack of solar illumination, or very low sun angles, during a large portion of the year. It is important to note that the availability of the composited radiances will allow other researchers to test and apply their own cloud algorithms, and users can implement a variety of improved, more potentially accurate approaches (such as multispectral statistical classifiers) for individual regions and times of year.

The basic cloud detection procedure used for the final release of APP products uses the Cloud and Surface Parameter (CASPR) procedures developed under EOS POLES funding, augmented by additional processing to take further advantage of the time history

available in the APP data set. See Appendix 2 for a detailed description of the procedure used. CASPR involves a combination of split-window and single-channel thresholds and temporal change detection using estimates of clear-sky surface temperature and albedo determined separately as a function of surface type. The final version of the APP products follows exactly the specific cloud detection steps outlined in the CASPR on-line documentation for the multi-day cloud detection method. As used for the APP processing, the initial part of the multi-day CASPR routine is done on 1/5 resolution data. The 5 km data is reduced to 25 kilometer to calculate the required means. This is done for efficiency, since the filling of missing (cloudy) areas from the closest clear areas is very computationally intensive, and little loss of statistical information occurs with the subsampling. The channel means are then magnified back to 5-km resolution for the final cloud masking in CASPR.

Because, in the standard CASPR approach, areas can be filled with "clear sky" values from locations that may not be representative at that location, an alternative method is used in conjunction with CASPR for the APP processing. A series of filters are applied to the AVHRR channel 4 time series to produce an estimated clear-sky surface temperature. This filtering operates as follows. Beginning with 365 days of twice-daily composited channel 4 brightness temperatures averaged to 25-km pixels, a combination of median and maximum filtering is applied to 20-day increments of the brightness temperatures for each pixel. The filtering picks the most likely clear-sky temperature for each pixel, and interpolates in time to fill in the estimated temperature during cloudy periods. This filtered series is used to produce a channel 4 mean, and the final CASPR cloud masking is redone using this mean.

This interpolated clear sky series is also used alone as a third cloud mask alternative. By differencing the daily channel 4 with the clear sky surface series and thresholding, a cloud mask is generated. The final cloud mask grid actually contains 3 cloud masks; multi-day CASPR, channel 4 comparisons only, and CASPR with the estimated channel 4 clear-sky means. In general, the latter, combined algorithm is likely to be most conservative in terms of whether a pixel is truly clear-sky or not (i.e., clear sky as indicated by this algorithm is most likely to be true clear sky). However, users are encouraged to examine the results of the three cloud masking algorithms for their particular region or application.

To date, the APP cloud masking has been evaluated using subjective methods designed to identify overall biases and problems. However, Figure 7 shows results of a comparison of an earlier version of the cloud mask product (clouds detected using the CASPR single-day algorithm) (Maslanik et al., 1999b).

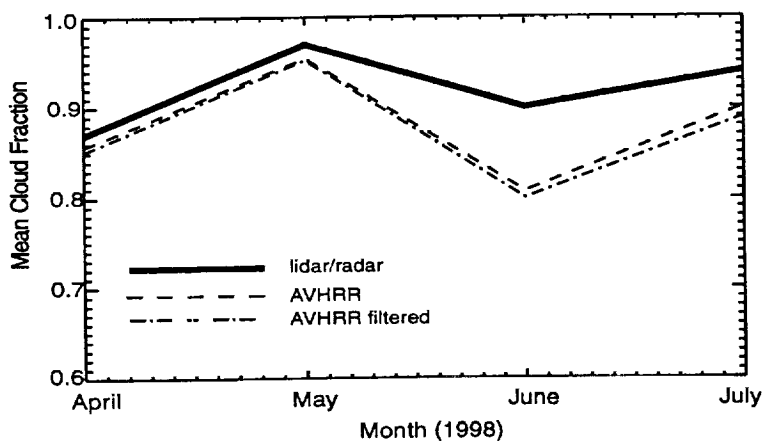


Figure 7. Monthly mean AVHRR-derived cloud fraction and cloud fraction observed by the NOAA LIDAR/RADAR at the SHEBA site. Means for the site location (individual 5-km pixel for AVHRR) (Maslanik et al., 1999b).

In this comparison, data from the surface-based lidar/radar system at the Surface Heat Budget of the Arctic (SHEBA) field project were used. The lidar/radar is considered to be very sensitive to all forms of cloud, relative to satellite remote sensing and observations obtained by surface observers. The initial comparison in Figure 7 may reflect this. These results and other work currently underway as part of a separate NASA-funded product-validation effort suggest generally good performance by the APP approach.

### 3.3.7. Surface Albedo and Skin Temperature

Figure 8 depicts the processing steps used to generate the APP geophysical products. Algorithms from the CASPR toolkit have been adapted to produce a clear-sky surface (skin) temperature from AVHRR channels 4 and 5, and a broadband albedo from channels 1 and 2 (see Appendix 2 and the on-line CASPR documentation for details). The surface temperature algorithm is a function of channel 4 and 5 brightness temperatures and scan angle and is based on simulations using the LOWTRAN radiative transfer model and Arctic radiosonde data and is similar to the procedure described by *Key et al. (1997)*.

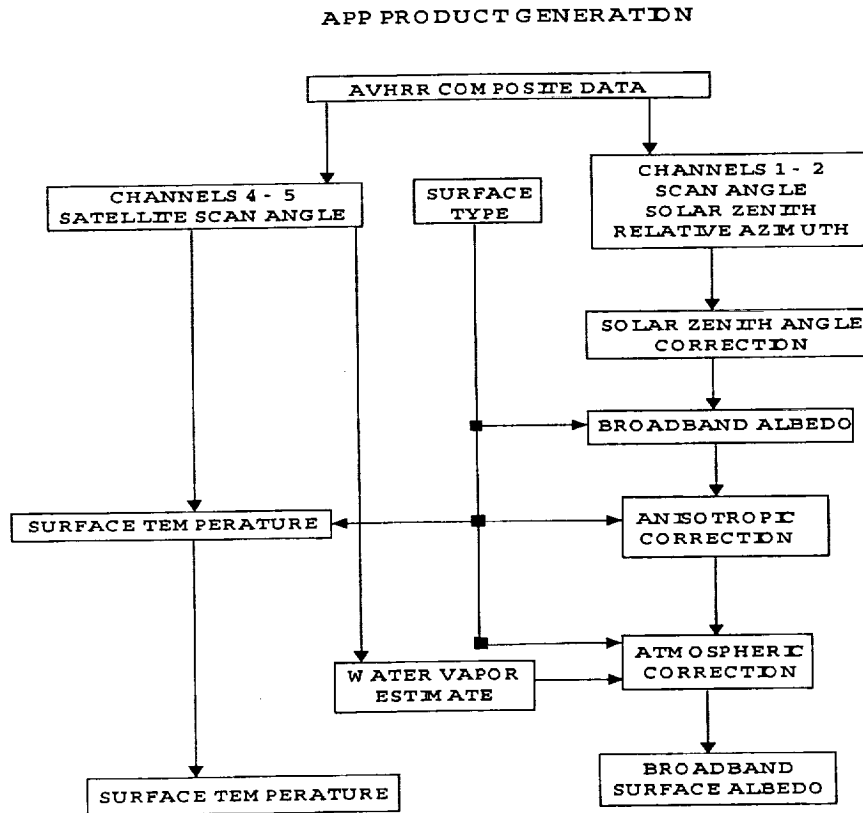


Figure 8. Processing steps for the generation of APP geophysical products (clear-sky surface temperature and clear-sky broadband surface albedo).

Top-of-the-atmosphere (TOA) AVHRR radiances are converted to surface albedo by first adjusting calibrated AVHRR channel 1 and channel 2 data to account for atmospheric attenuation and bi-directional reflectance, and then converted to broadband albedos. Figures 2 and 3 showed examples of the 5-km broadband albedo and skin temperature products.

These algorithms are intended for clear-sky areas. However, we have chosen to apply them to all pixels rather than to only those pixels flagged as clear-sky using the cloud masking routines. The reasoning for this is three-fold: First, the cloud detection algorithm can be used in a variety of different ways by selecting among the cloud-detection flags supplied by the three algorithm versions used (see previous section). Also, cloud detection algorithms continue to evolve and improve. Users can therefore continue to take advantage of the APP geophysical products by applying alternative algorithms. For example, users can apply refined methods, including manual interpretation, that can be tuned to maximize performance for specific regions and case studies. These custom cloud masks can then be applied to the APP skin temperature and surface albedo product, without the need for users to implement their own surface product algorithms. Third, some users may wish to investigate the usefulness of the surface products under marginal cloud conditions - conditions that may be detected by AVHRR as being cloudy, but which may actually consist of very thin cloud or diamond dust precipitation. We must emphasize, however, that since the CASPR surface algorithms will not work properly for cloudy pixels, the APP clear-sky skin temperature and albedo grids contain inaccurate values. As noted above, users need to apply either the provided cloud mask or their own cloud detection interpretation.

Evaluation of the CASPR surface products and the cloud detection approach is ongoing, and in the process, we identified several shortcomings of the original "version 1" products. As noted in Section 2, processing was delayed in order to develop and implement improvements to the original product algorithms. Tests also indicate that performance of the standard albedo algorithm over ice sheets still warrants improvement. The accuracy of the model simulations that form the basis of the CASPR albedo algorithm decreases with low solar zenith angles (e.g., the sun low on the horizon). Thus, albedos calculated in spring and autumn are likely to be less accurate than those for time periods with higher sun angles. Also, the parameterizations used to address bi-directional reflectance are not equally representative of all snow conditions for a full range of sun angles and satellite viewing angles.

Figure 9 illustrates typical results from ongoing comparisons of the APP products and products derived from the APP radiance data to field measurements. In this case, the results of comparisons to SHEBA field measurements include additional CASPR-derived geophysical products such as all-sky albedo and skin temperature and down-welling radiative fluxes. The results indicate that the basic level of accuracy for retrievals over sea ice are reasonable. Other tests over the Greenland ice sheet suggest larger errors in the broad-band albedo estimates, probably arising from the sensitivity of the algorithm used to low sun angles in combination with a reduced atmospheric column depth and the decreased representativeness of the algorithm's parameterizations for high-elevation surfaces.

### 3.3.8 Ice Motion

The APP ice motion products complement existing drifting buoy data from the International Arctic Buoy Program (IABP) and provide an historical record of ice motion prior to the availability of RADARSAT-derived ice products. Using corresponding passes for consecutive days, daily sea-ice displacement vectors are determined through image-to-image correlation (*Emery et al., 1991; 1995*). Ice velocities estimated from the 5-km AVHRR channel composites are mapped to a 50 km grid (25 km grid for 1.25-km data), and to a 62.5 km grid for passive microwave-derived motions and blended motions consisting of merged AVHRR-, passive microwave- and buoy-derived ice motions. Characteristics of the sea-ice motion products dictate a different processing strategy and format than is used for the twice-daily products noted above. For each day, four scenes are chosen with acquisition times near 0000, 0600, 1200 and 1800 GMT. These times allow for complete coverage of the polar ice with some overlap and also compares as well as possible to the 12-hourly IABP buoy data.

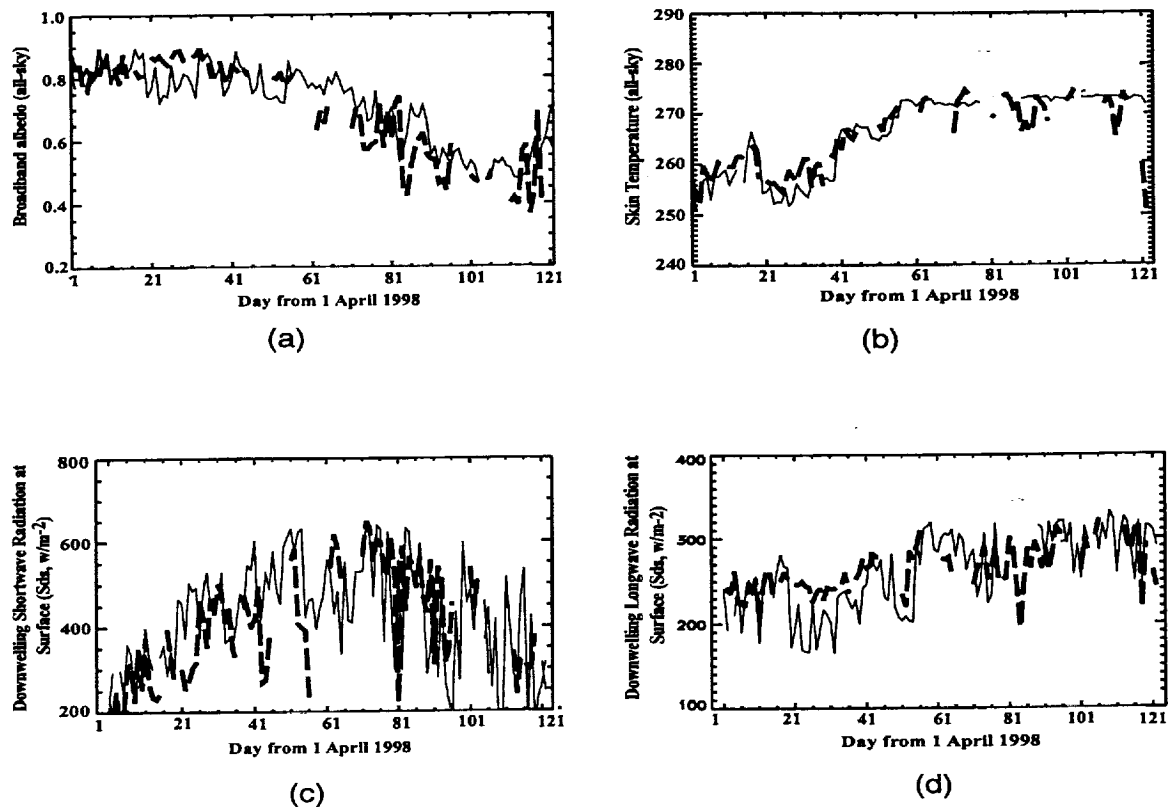


Figure 9. Comparison of daily (nominal 1400 hr. local time) AVHRR-derived time series and field-measured data for surface all-sky broadband albedo (a), all-sky skin temperature (b), downwelling shortwave radiation at the surface (c), and downwelling longwave radiation at the surface (d). The thick dashed line represents AVHRR data. The thin line represents surface measurements. Products are calculated from APP composited radiances (Maslanik *et al.*, 1999b).

Given the extensive cloudiness in the polar regions, the requirement that clear-sky conditions exist for consecutive days is a major limitation of AVHRR for mapping ice motion. An additional APP ice motion product will therefore be generated by combining AVHRR-derived ice displacements with other ice motion information via optimal interpolation to create ice-motion fields that are uniform in time and space. These "blended" motion fields will include ice-motion information extracted from AVHRR, drifting buoys, and passive microwave data (SMMR and SSM/I) (Agnew *et al.*, 1997; Emery *et al.*, 1997; Liu and Cavalieri, 1998; Kwok *et al.*, 1998). The blended motion field thus takes advantage of the accurate but sparse buoy motions, the detailed but intermittent AVHRR-derived motions, and the lower-resolution but uniform temporal coverage provided by the passive microwave sensors. SSM/I- and SMMR-derived ice displacements are estimated using the same modified maximum cross-correlation and combination technique used for AVHRR processing. Displacements are calculated over a 24-hour period using daily-averaged grids of 85 GHz and 37 GHz brightness temperatures obtained from NSIDC. Retrieval of these microwave-derived motions is hindered by atmospheric water content and surface melt during late spring through early autumn. During other times, comparisons with drifting buoys indicate that the motions exhibit little bias in the Arctic, with a standard deviation of 5 to 6 cm/s for the daily displacements relative to buoys. Preliminary analysis indicates larger errors for the Southern Ocean, with a general underestimation of drift speed

using the passive microwave data. Error standard deviation for the 5-km ice-motion products is approximately 2 cm/sec for AVHRR-derived vectors. For the APP products, the motion data sets will include blended motions from AVHRR, SMMR, SSM/I and buoys, as well as individual, un-blended sets of the AVHRR- and passive microwave-derived motion data.

### 3.3.9 Latitude/Longitude Values

Grids of latitude/longitude coordinates (the estimated center location of each pixel) are provided. These are provided as floating-point ASCII text values, organized as an image of the same dimensions of the Northern and Southern Hemisphere grids. Values are stored as fractions of degrees. Separate grids are provided for latitude and longitude.

### 3.3.10 25-km products

Selected 5-km APP products are averaged into 25-km grid cells, providing browse products for the northern and southern hemispheres. These reduced-resolution products also provide a means of analyzing conditions and trends at a more manageable data volume. The available 25-km products include reduced-resolution versions of albedo, skin temperature, and the cloud mask. All the values are sub-sampled, but the cloud mask also includes cloud fraction estimated from the cloud/no-cloud pixels within the 5 pixel x 5 pixel window used to convert from 5-km to 25-km pixels.

## 3.4 *File Format and File Naming Convention*

The data format as supplied to NSIDC is in "flat binary" format, with number of bytes and scaling as given in Tables 2 and 3. Each parameter is stored as a separate file. See [http://www-nsidc.colorado.edu/NASA/GUIDE/EASE/ease\\_maps\\_info.html](http://www-nsidc.colorado.edu/NASA/GUIDE/EASE/ease_maps_info.html) for a description of EASE-Grid map projection and grid parameters used for the APP project. Also, see the on-line NSIDC documentation for additional information.

The file naming convention used is consistent with that for the other Polar Pathfinder projects, and is designed to carry a maximum amount of information for easy identification of data types. These files are of three types: raster files, text files, and ice motion vector files. The file naming convention is as follows:  
Raster files have filenames of the form

□ app\_H001\_YYYYDDD\_HH00\_ZZZZ.vX.gz

where

- H is the hemisphere (n or s)
- YYYY is the year
- DDD is the day of year
- HH is the hour (04 or 14 for north files, 02 or 16 for south files)
- ZZZZ is the file type as follows:

■ 2 byte gzipped raster files:

■ albd - surface albedo (0.1 per cent, range 0 to about 1000)

- chn1 - AVHRR channel 1 (0.1 per cent, range 0 to about 1000)
- chn2 - AVHRR channel 2 (0.1 per cent, range 0 to about 1000)
- chn3 - AVHRR channel 3 (0.1 K, range about 1900 to about 3100)
- chn4 - AVHRR channel 4 (0.1 K, range about 1900 to about 3100)
- chn5 - AVHRR channel 5 (0.1 K, range about 1900 to about 3100)
- sael - satellite elevation angle (0.1 degree, range 0 to 900)
- solz - solar zenith angle (0.1 degree, range 0 to 900)
- reaz - relative azimuth angle (0.1 degree, range 0 to 1800)
- temp - surface temperature (0.1 K, range about 1900 to about 3100)
- 1 byte gzipped raster files:
  - amsk - AVHRR-derived ice mask and land/water mask. The bits in this mask have the following layout:
    - bit 7 - valid data
      - 0: invalid or missing data
      - 1: valid data
    - bit 6 - AVHRR-derived ice:
      - 0: not ice
      - 1: ice
    - bit 3 - Land/water:
      - 0: water
      - 1: land
    - bits 5, 4, 2, 1, and 0 are always 0

■ for invalid or missing data, all bits are 0 (i.e. amsk = 0)

■ NOTE: the amsk file is an intermediate file which is used as input to the temperature, albedo, and cloud masking procedures. Bits 6 and 3 data in amsk are copied to the same bit positions in the cmsk file described below. The amsk file is archived to the timberwolf for use in recomputing the temperature, albedo, and/or cloud mask as needed.

■ cmsk - cloud mask. The bits in this mask have the following layout:

■ bit 7 - Cloud

■ 0: clear

■ 1: cloud

■ bit 6 - AVHRR-derived ice:

■ 0: not ice

■ 1: ice

■ bit 5 - SSMI-derived ice:

■ 0: not ice

■ 1: ice

■ bit 4 - SSMI-LOCI-derived coastline:

■ 0: not coastline

■ 1: coastline

■ bit 3 - Land/water:

■ 0: water

■ 1: land

■ bits 2, 1, 0 - Region number in the range 0 to 7

■ bits 5 and 4 are never both 1 for valid data

■ bits 5 through 0 comprise a domain in

the range 0-47 used in the cloud masking procedure

■ for invalid or missing data, all bits are 1 (i.e. cmsk = 255)

■ omsk - orbit mask (input scene code, range 0 to 14)

■ time - GMT time of acquisition (0.1 hour, range 0 to about 244)

□ X is a version number (range 0 to 9)

Also included with each set of raster files is a small text file (<1000 bytes):

- app\_H001\_YYDDD\_HH00\_info.vX - mask text file

The dimensions of the raster files are: 7220x7220 for north files = 104 Mb 2 byte and 52 Mb 1 byte (unzipped) 6420x6420 for south files = 82 Mb 2 byte and 41 Mb 1 byte (unzipped).

Ice motion vector files have filenames of the form:

- app\_H001\_YYDDD\_HH00\_icem.vX.gz

where

□ HH is 00, 04, 08, 12, 16, 20, or 24.

Thus, depending on data availability, up to 7 ice motion files may be created for a particular day for each hemisphere.

#### 4. Contacts

AVHRR Polar Pathfinder Investigators:

James Maslanik  
Colorado Center for Astrodynamics Research  
Campus Box 431  
University of Colorado  
Boulder, CO 80309  
303-492-7221  
jimm@kryos.colorado.edu

Chuck Fowler  
Colorado Center for Astrodynamics Research  
Campus Box 431  
University of Colorado  
Boulder, CO 80309  
303-492-0975  
cfowler@boulder.colorado.edu

Ted Scambos  
National Snow and Ice Data Center  
CIRES, Campus Box 449  
University of Colorado  
Boulder, CO 80309  
303-492-1113  
teds@kryos.colorado.edu

Terry Haran  
National Snow and Ice Data Center  
CIRES, Campus Box 449  
University of Colorado  
Boulder, CO 80309  
303-492-1847  
tharan@kryos.colorado.edu

Primary Contact for the AVHRR data sets:

User Services  
National Snow and Ice Data Center  
CIRES, Campus Box 449  
University of Colorado  
Boulder, CO 80309  
303-492-6199  
nsidc@kryos.colorado.edu

## 5. REFERENCES

- Agnew, T.A., H. Le, and T. Hirose, 1997. Estimation of large scale sea ice motion from SSM/I 85.5 GHz imagery, *Annals of Glaciol.*, 25, 305-311.
- Armstrong, R.L. and M.J. Brodzik. 1995. An Earth-gridded SSM/I data set for cryospheric studies and global change monitoring. *Adv. Space Res.* 16(10):155-(10)163.
- Csiszar, I. and G. Gutman, 1999, Mapping global land surface albedo from NOAA AVHRR, *J. Geophys. Res.*, 104(D6), 6215-6228.
- Emery, W.J., C.W. Fowler, J. Hawkins, and R.H. Preller. 1991. Satellite image inferred sea ice motion in Fram Strait, the Greenland Sea and the Barents Sea, *J. Geophys. Res.*, 96(C5), 15 May, 8917-8920, 1991.
- Emery, W.J., C.W. Fowler, J.A. Maslanik, 1995, Satellite remote sensing of ice motion, In: *Oceanographic Applications of Remote Sensing*, M. Ikeda and F.W. Dobson (eds.), CRC Press, Boca Raton, 367-379.
- Emery, W.J., C. Fowler, and J.A. Maslanik, 1997. Satellite-derived maps of Arctic and Antarctic sea ice motion: 1988 to 1994. *Geophys. Res. Lett.*, 24, 8, 897-900.
- Fowler, C., J.A. Maslanik, and W.J. Emery, 1994. Observed and simulated ice motion for an annual cycle in the Beaufort Sea, IGARSS '94, Pasadena, CA, 1303-1305.
- Gustafson, G.B. et al., 1994, Support of Environmental Requirements for Cloud Analysis and Archive (SERCAA), Phillips Laboratory, Hanscom Air Force Base, Scientific Report No. 2, PL-TR-94-2114,; 100 pp.
- Hutchinson, T.A. and T.A. Scambos, 1997. High-resolution polar climate parameters derived from 1-km AVHRR data, *Am. Met. Soc.*, 8th. Conf. on Global Change Studies, 284-291.
- Key, J., 1999, The cloud and surface parameter retrieval (CASPR) system for polar AVHRR. Cooperative Institute for Meteorological Satellite Studies, University of Wisconsin, Madison, 59 pp.

- Key, J. and J. Intrieri, 1999, Cloud particle phase determination with the AVHRR, *J. Appl. Meteorol.*, submitted November 1999.
- Key, J. and A.J. Schweiger, 1998, Tools for atmospheric radiative transfer: Streamer and FluxNet. *Computers and Geosciences*, 24(5), 443-451.
- Key, J., J. Collins, C. Fowler, and R.S. Stone, 1997, High-latitude surface temperature estimates from thermal satellite data, *Remote Sensing Environ.*, 61: 302-309.
- Key, J. 1996. Cloud and surface parameter retrieval (CASPR) system for polar AVHRR: User's guide. Technical Report 96-02, Boston, MA, Boston University, Department of Geography, Boston Univ., (Technical report 96-02.)
- Kwok, R., A. Schweiger, D.A. Rothrock, S. Pang, and C. Kottmeier, 1998. Sea ice motion from satellite passive microwave imagery assessed with ERS SAR and buoy motions. *J. Geophys. Res.*, vol. 103, C4, 8191-8214.
- Liu, A.K. and D.J. Cavalieri, 1998. On sea ice drift from the wavelet analysis of the Defense Meteorological Satellite Program (DMSP) Special Sensor Microwave Imager (SSM/I) data. *Int. J. Remote Sensing*, vol. 19, no. 7, 1415-1423.
- Maslanik, J., C. Fowler, J. Key, T. Scambos, T. Hutchinson, and W. Emery, 1998. AVHRR-based Polar Pathfinder products for modeling applications. *Annals of Glaciol.*, 25, 388-392.
- Maslanik, J.A., A. Lynch, and C. Fowler, 1999a. Assessing 2-D and coupled-model simulations of sea ice anomalies using remotely-sensed polar pathfinder products, Fifth Conference on Polar Meteorology and Oceanography, Am. Met. Soc., Dallas, TX, 10-15 January, 476-479.
- Maslanik, J.A., J. Key, C. Fowler, T. Nguyen, and X. Wang, 1999b. Spatial and Temporal Variability of Satellite-derived Cloud and Surface Characteristics During FIRE-ACE, submitted to *Journal of Geophysical Research*, November, 1999.
- Meier, W.N., J.A. Maslanik, J.R. Key, and C.W. W. Fowler, 1997. Multiparameter AVHRR-derived products for Arctic climate studies, *Earth Interactions*, Vol. 1.
- NOAA, 1991, *NOAA Polar Orbiter Data User's Guide*, U.S. Dept. of Commerce., National. Ocean. and Atmos. Admin., NESDIS, February.
- Rao, C.R.N., 1993. Nonlinearity corrections for the thermal infrared channels of the AVHRR: Assessment and recommendations. NOAA Tech. Rept., NESDIS 69, 31 pp.
- Rao, C.R.N. and J. Chen, 1999. Revised post-launch calibration of the visible and near-infrared channels of the Advanced Very High Resolution Radiometer (AVHRR) on the NOAA-14 spacecraft, *Int. J. Rem. Sens.*, 20, 18, 3485-3491.
- Rosborough, G.W., D.G. Baldwin, and W.J. Emery, 1994. Precise AVHRR image navigation. *IEEE Trans. Geosci. and Remote Sens.*, 32, 3, 644-657.
- Saunders, R.W. and K.T. Kriebel, 1988, An improved method for detecting clear sky and cloudy radiances from AVHRR data, *Int. J. Remote Sensing*, 9(1), 123-150.
- Schweiger, A.J. and J.R. Key, 1992. Arctic cloudiness: Comparison of ISCCP-C2 and Nimbus-7 satellite-derived cloud products with a surface-based cloud climatology, *J. Climate*, 5, 12, 1514-1527.
- Schweiger, A., C. Fowler, J. Key, J. Maslanik, J. Francis, R. Armstrong, M.J. Brodzik, T. Scambos, T. Haran, M. Ortmeier, S. Khalsa, D Rothrock, and R. Weaver, 1999. P-Cube: A multisensor data set for polar climate research. Proc. 5th. Conf. on Polar Meteorology and Oceanography, American Meteorological Society, Dallas, TX, 15-20 Jan., 136-141.
- Schweiger, A.J., M.C. Serreze, and J.R. Key, 1993, Arctic sea ice albedo: A comparison of two satellite-derived data sets, *Geophys. Res. Lett.*, 20, 1, 41-44.
- Stowe, L.L., E.P. McClain, R. Carey, P. Pellegrino, and G.G. Gutman, 1991, Global distribution of cloud cover derived from NOAA/AVHRR operational satellite data, *Adv. Space Res.*, 11(3), 51-54.
- Sullivan, J. 1999. New radiance-based method for AVHRR thermal channel nonlinearity corrections, *Int. J. Rem. Sens.*, 20, 18, 3493-3501.
- Suttles, J.T., R.N. Green, P. Minnis, G.L. Smith, W.F. Staylor, B.A. Wielicki, I.J. Walker,

D.F. Young, V.R. Taylor, and L.L. Stowe, 1988, Angular radiation models for Earth-Atmosphere system. Volume I-Shortwave radiation, *NASA Reference Publication 1184*, 144 pp.

## APPENDIX 1. DISCUSSION OF CALIBRATIONS AND ADJUSTMENTS

Since the best available calibration evolved during the life of the project, the APP composited radiances produced during part of the project were generated using one calibration approach, while later data were processed using improved calibrations. Data processed using the earlier version and which have been adjusted using the corrections described below are identified as Version 1, while the latter data processed using the final calibrations are identified as Version 2. The corrections applied for the Version 1 data yield values very close to those achieved using the final calibrations.

The following text is taken from the on-line documentation available at <http://polarbear.colorado.edu/app-calibration.html>. Please use the online version to access the links indicated in the text below.

### Comparison of the calibration methods

The thermal channel calibration outlined in the Polar Orbiter Users guide, and which was used for the Version 1 processing, is as follows:

- compute a linear slope and intercept based upon the instrument count of space and internal black body,
- apply the slope and intercept to calculate scene radiance,
- convert the radiance to brightness temperature using the Plank functions,
- and finally, apply a non-linear correction to the temperatures using a look-up table of corrections based upon scene and black-body temperature.

This method was optimized by NOAA for sea surface temperature products, which essentially means that the calibrations were best suited for warmer regions.

The newly applied method (used for version 2) applies the non-linear correction to the radiance, before the brightness temperature. This non-linear correction consists of a quadratic function, with coefficients derived from pre-flight calibrations. The results, while not optimized for the narrower range needed for the sea surface temperature products, appear to be an improvement for the much wider range needed for the areas covered by the Polar Pathfinder products.

### Problems and Bugs in the Original Implementations

- No non-linear corrections were done for NOAA-7. The NOAA look-up tables were not available at the time the calibration programs were written.
- The central wave number for channel 4 was found to have been changed in the current NOAA documentation.
- A problem in calibration of NOAA-14 thermal channels was discovered in the calibration software. The first 50 scan lines were calibrated incorrectly, but the remainder of the orbit was not done properly.
- Some other parameters were found that had changed, but had no, or very small, effects on the final products (less than 0.1 degrees).

### Corrections to the Already Processed Products

Since it was not feasible to re-process all of the Version 1 data that had been calibrated using the original methods, correction tables were generated by comparing the old vs. new methods. In most cases, these adjustments correct the data to 0.0 +/- 0.1 degrees error, relative to the version 2 calibration method. These corrections have been applied to all processed channel 4 and 5 data (the Version 1 data) from NOAA-7, 9, 11, 12, and 14 satellites. Corrections were also be applied to channel 3 of NOAA-14.

The on-line version of this appendix includes links to the look-up tables for the correction values that were applied to the already processed data to match the newer calibration methods. These tables contain 1301 correction values every 0.1 degree from 180 K to 310 K. The corrections are degrees x 10. Therefore, a value of 100 would be a correction of 10.0 degrees. The on-line text also includes additional plots and summaries of the comparisons.

### Summary of Results by Channel

Channel 3: This only applies to NOAA 14. The corrections are quite large, up to 18 degrees.

Channel 4: The corrections for NOAA-7,9,11, and 12 are very similar, with little correction except at the lowest temperatures, where the corrections are about 1 degree. Again, with NOAA-14, the correction is large as with channel 3, with corrections ranging from -15 to 1 degrees.

Channel 5: Results are similar to Channel 5. NOAA-7,9,11,and 12 corrections range from -1.0 to just above 0.0 degrees. NOAA-14 ranges from -5 to 0.5 degrees.

### Summary of Results by Satellite

#### **NOAA-7**

Channel 4 corrections range from 1.5 at 180 K to -1.0 at 250 K and to 0.8 at 210 K.

Channel 5 values range from -1.0 at 180 K to 0.6 at 310 K.

The values are somewhat larger than the corrections to NOAA-9, 11, and 14 because no non-linear corrections had been previously applied.

#### **NOAA-9**

Similar to NOAA-7, but correction values less. Channel 4 ranges from 1.0 at 180 K to -0.2 at 310 K.

No correction for channel 5.

#### **NOAA-11**

Channel 4 correction values range from 1.5 at 180 K to -0.2 at 310 K.

Channel 5 values are from -.01 at 180 K to 0.3 at 310 K.

#### **NOAA-12**

Essentially no corrections for channels 4 or 5 above 220 K.

Below 220 K, channel 4 values are up to 1.2 at 180 K, and channel 5 are to -0.9 at 180 K.

## NOAA-14

Because the calibration of NOAA-14 had been done incorrectly, the values are quite large. Channel 3 ranges from 18.0 at 180 K to 0 at 310 K. The instrument seems to saturate at 200 K and reliable correction values were impossible to obtain below 200 K. Channel 4 varies from -14 at 180 K to ~0 at 310 K. Channel 5 is from -6 at 180 K to 0 at 310 K.

## APPENDIX 2. DESCRIPTION OF SATELLITE ALGORITHMS

In this section the algorithms used to detect clouds and to estimate surface properties from AVHRR for the APP processing are briefly described. See *Key* (1999) for additional details and references.

In addition to the calibrations noted above, channels 1 and 2 are further adjusted for Earth-Sun distance. At 3.7  $\mu\text{m}$ , AVHRR channel 3 contains both reflected solar and emitted thermal components. The reflected portion is approximated by removing from the total radiance an estimate of the emitted portion, based on the temperature of channel 4:

$$\rho_3 = \frac{L_3 - B_3(T_4)}{L_0\mu - B_3(T_4)} \quad (\text{A1})$$

where  $\rho_3$  is the channel 3 reflectance,  $L_3$  is the channel 3 radiance,  $B_3(T_4)$  is the Planck function for channel 3 based on the channel 4 temperature  $T_4$ ,  $L_0$  is the solar constant for the band (adjusted for Earth-Sun distance), and  $\mu$  is the cosine of the solar zenith angle.

### Surface Temperature

For the retrieval of clear sky surface temperature a simple regression model is used to correct for atmospheric attenuation. For high-latitude ocean and snow-covered land we use the equation

$$T_s = a + bT_4 + c(T_4 - T_5) + d[(T_4 - T_5)(\sec\theta - 1)] \quad (\text{A2})$$

where  $T_s$  is the surface temperature,  $T_4$  and  $T_5$  are the satellite measured brightness temperatures in channels 4 and 5,  $\theta$  is the sensor scan angle, and  $a$ ,  $b$ ,  $c$ , and  $d$  are regression coefficients. To determine the empirical relationship radiosonde data from drifting ice and land stations in the Arctic and Antarctic were used with a radiative transfer model to simulate the sensor brightness temperatures. The surface temperature retrieval methods for both sea ice/snow and snow-free land are described in detail in *Key, et al.* (1997) and is provided in the on-line documentation.

### Surface Albedo

The retrieval of surface albedo involves four steps: (1) convert channels 1 and 2 narrowband reflectances to a broadband reflectance, (2) correct the top-of-atmosphere (TOA) broadband reflectance for anisotropy, (3) convert the TOA broadband albedo to a surface broadband albedo, and (4) adjust the surface clear sky broadband albedo for the effects of cloud cover in cloudy pixels. The general methodology described by steps 1-3 was used by *Csiszar and Gutman* (1999) for global land studies. For this study relationships for land and ocean were developed independently, and methods for snow/ice

and ocean were added. The albedo presented here is a directional-hemispherical, apparent albedo, where "apparent" albedo is what would be measured by up- and down-looking radiometers in the field. In other words, the calculated surface albedo varies with atmospheric conditions and the solar zenith angle.

The first step is to convert the narrowband reflectances in AVHRR channels 1 and 2 to a top-of-atmosphere (TOA) broadband reflectance. The narrow-to-broadband conversion takes the form

$$\rho_{toa} = a + b\rho_{1,toa} + c\rho_{2,toa} \quad (A3)$$

where  $\rho_{1,toa}$  is the channel 1 reflectance,  $\rho_{2,toa}$  is the channel 2 reflectance,  $\rho_{toa}$  is the broadband TOA reflectance, and  $a$ ,  $b$ , and  $c$  are regression coefficients. To develop the regression relationship the radiative transfer model *Streamer* (Key and Schweiger, 1998) was used to simulate the TOA reflectances over a broad range of viewing and illumination angles, atmospheric conditions, and surface types and albedos. Separate sets of coefficients were determined for different surface types.

The next step is to correct for the dependence of the sun-satellite-surface geometry on reflectance. This is done with data presented in *Suttles et al.* (1988), who used ERBE and GOES data to determine TOA anisotropic reflectance factors (ARF) for the broad shortwave band over various surfaces. To convert the directional reflectance to albedo, the ERBE/GOES ARFs are used:

$$\alpha_{toa} = \frac{\rho_{toa}}{f} \quad (A4)$$

where  $\rho_{toa}$  is the reflectance observed at the sensor (simulated by *Streamer* in step 1),  $f$  is the anisotropic reflectance factor, and  $\alpha_{toa}$  is the TOA albedo, which is only a function of solar zenith angle.

Next, the broadband, clear sky, apparent surface albedo is estimated with a regression relationship of the form

$$\alpha_{toa} = a + b\alpha_s \quad (A5)$$

where  $\alpha_s$  is the surface reflectance, and  $a$  and  $b$  are a function of water vapor, aerosol amount, and solar zenith angle. The coefficients were determined with *Streamer* for a variety of surface and atmospheric conditions.

## Cloud Detection

The cloud masking procedure consists of thresholding operations that are based on modeled sensor radiances. The AVHRR radiances are simulated (using *Streamer*) for a wide variety of surface and atmospheric conditions, and values that approximately divide clear from cloudy scenes are determined. The daytime and nighttime algorithms have very different logic. In the presence of sunlight (daytime), the spectral cloud tests work well in that false detections (labeling clear pixels as cloudy) are infrequent. So the daytime algorithm uses only spectral tests and is conceptually simple: initialize the cloud mask to clear, then apply the cloud tests to label cloudy pixels.

In the absence of sunlight the procedure is different because there is less spectral information available and because AVHRR channel 3 tends to be noisy at low temperatures, common during the polar night. Under most conditions optically thick clouds simply cannot be distinguished from clear sky with the three thermal channels alone. The nighttime

different logic. In the presence of sunlight (daytime), the spectral cloud tests work well in that false detections (labeling clear pixels as cloudy) are infrequent. So the daytime algorithm uses only spectral tests and is conceptually simple: initialize the cloud mask to clear, then apply the cloud tests to label cloudy pixels.

In the absence of sunlight the procedure is different because there is less spectral information available and because AVHRR channel 3 tends to be noisy at low temperatures, common during the polar night. Under most conditions optically thick clouds simply cannot be distinguished from clear sky with the three thermal channels alone. The nighttime algorithm first applies the spectral cloud tests, resulting in some false detections for noisy pixels and for optically thick clouds. The spectral test thresholds are set to be clear-conservative to increase the likelihood that those pixels labeled as clear are in fact clear. Next a clear sky channel 4 temperature image is constructed by passing a mean filter over the clear pixels, eliminating much of the noise and false detections. The image is then rethresholded based on the clear sky map such that temperature departures more than some number of degrees from the clear sky mean signifies that a pixel is cloudy. In this final thresholding it is possible for the cloud to be either warmer or colder than the surface, especially during the winter.

Many of the cloud test concepts can be found in the Air Force SERCAA procedures (Gustafson et al., 1994); some appear in the NOAA CLAVR algorithm (Stowe et al., 1991); most were developed and/or used elsewhere. In the discussion below, "warm" cloud refers to clouds that have higher temperatures than the surface, while "cold" clouds have temperatures lower than the surface. The cloud tests are:

1. Cirrus test, 11-12  $\mu\text{m}$  (day and night) - A pixel is cloudy if  $\text{BTD45} > \text{CCT\_TABLE}$ , where BTD45 is channel 4 minus channel 5 brightness temperature difference and CCT\_TABLE is a table of thresholds from *Saunders and Kriebel* (1988), extended to include lower temperatures (range: 230-310 K). The thresholds are the expected maximum BTD45 for clear sky.
2. Warm clouds, 11-12  $\mu\text{m}$  (day and night) - For warm clouds BTD45 may be negative so an additional test is required (cf., *Yamanouchi et al.*, 1987). A pixel is considered to be cloudy if  $\text{BTD45} < \text{WARM45}$ . This test is most applicable at night in the presence of a temperature inversion.
3. Water cloud test, 3.7  $\mu\text{m}$  (day only) - A pixel is considered cloudy if  $\text{REF3} > \text{REF3\_THRESH}$  and  $\text{REF1} > \text{REF1\_THRESH}$ , where REF1 and REF3 are the channels 1 and 3 reflectances and REF1\_THRESH and REF3\_THRESH are threshold values.
4. Low stratus, thin cirrus tests, 3.7-11  $\mu\text{m}$  (night only) - A pixel is cloudy if  $\text{BTD34} \leq \text{LSTTCI\_34LO}$  or  $\text{BTD34} \geq \text{LSTTCI\_34HI}$ , where BTD34 is the brightness temperature difference between channels 3 and 4.

CASPR includes a single-day and multi-day implementation of this approach. The multi-day method was used for the APP processing. The multi-day method operates as follows. The time series cloud masking procedure operates on a sequence of images acquired on consecutive days at approximately the same solar time. It first applies the spectral tests for an initial labeling of cloudy and clear pixels, then further refines the identification of clear pixels by examining changes in spectral characteristics from one day to the next. The clear pixels that result from these spectral and temporal tests are used to construct a clear sky radiance statistics over some number of days for various spectral channels. The statistics are then used in a final thresholding operation to label/re-label pixels as either clear or cloudy. More specifically the steps are:

1. Apply the spectral tests of the single-image cloud mask procedure in a clear conservative mode, so that those pixels labeled as clear most likely are. See 'cldmask1.pro' for details.

2. Examine the time change in spectral characteristics between pairs of days. A pixel is clear if the spectral tests (step #1) say it is clear, and if it varies little from one day to the next. The channel 4 brightness temperature and the adjusted brightness temperature difference (4-5) are used in the time tests when any part of the image is dark; the channel 4 brightness temperature, the channel 1 reflectance, and the channel 3 reflectance are used during the day.

3. Clear sky statistics are compiled for each pixel using all clear values within some distance of the pixel and over some number of days (typically 9x9 pixel cells and 5 days, see the keywords 'ndays' and 'cellrad'). Means and standard deviations of the channels 1 and 3 reflectances (day only) and the channel 4 temperature (day and night) are computed. If a cell occurs along a coastline, only pixels with the same surface type (LAND or NOTLAND) as the center pixel are used. Pixels in the clear sky composite that did not have means and standard deviations assigned due to the lack of clear values are filled by bilinear interpolation. The probability of finding clear pixels can be increased by enlarging the cell size or using more days, but doing so also increases the variability.

4. The clear sky composite means are used in a threshold operation to label or re-label all pixels as clear or cloudy. A pixel can be labeled as cloudy if its brightness temperature respectively, some value that represents its natural variability, or if its reflectance in either channel 1 or 3 is higher than its mean clear reflectance plus (not minus) some other value. If any part of the image is dark, the nighttime final thresholding is done on the entire image, though both the daytime and nighttime spectral cloud tests are used in the initial labelling (step #1).

See the on-line CASPR Reference Guide at the web site location given earlier for a description of the sources of these cloud tests. Most of these tests are found in the Air Force SERCAA (Gustafson et al., 1994) operational cloud analysis procedure, some are in NOAA CLAVR (Stowe et al., 1991); almost all have been used and/or developed by others.